Supplemental Figures

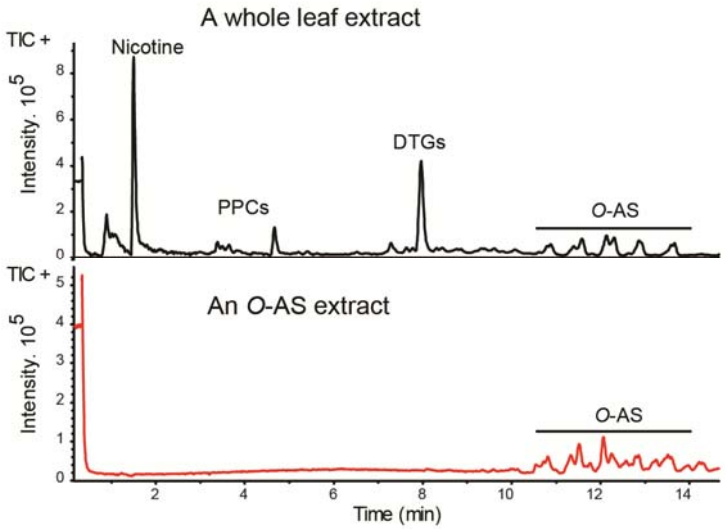

Figure S1. Total ion chromatogram of a positive mode UHPLC/TOF-MS run (TIC+) of a whole leaf extract which is compared with an *O*-acyl sugars (*O*-AS) extract. The leaf extract is dominated by nicotine, phenylpropanoid polyamine conjugates (PPCs), 17-hydroxygeranyllinalool diterpene glycosides (DTGs), and *O*-AS, while the *O*-AS extract was dominated by a mixture of *O*-AS.

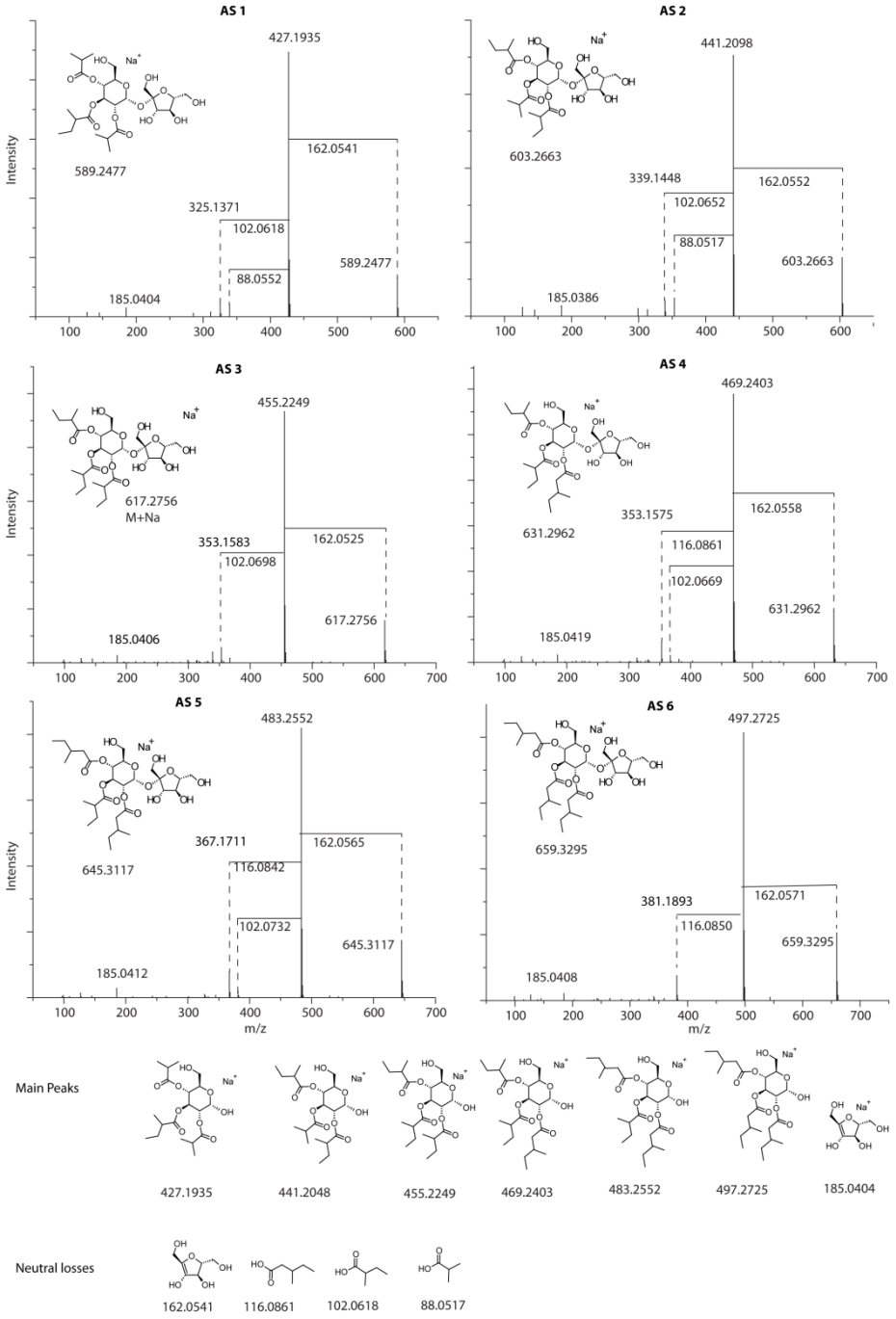

Figure S2: MS^2 spectra of class 2 *O*-acyl sugars and the annotation of the main fragment peaks (Main peaks) and neutral losses. The position of the branched-chain fatty acids could not be verified and may vary.

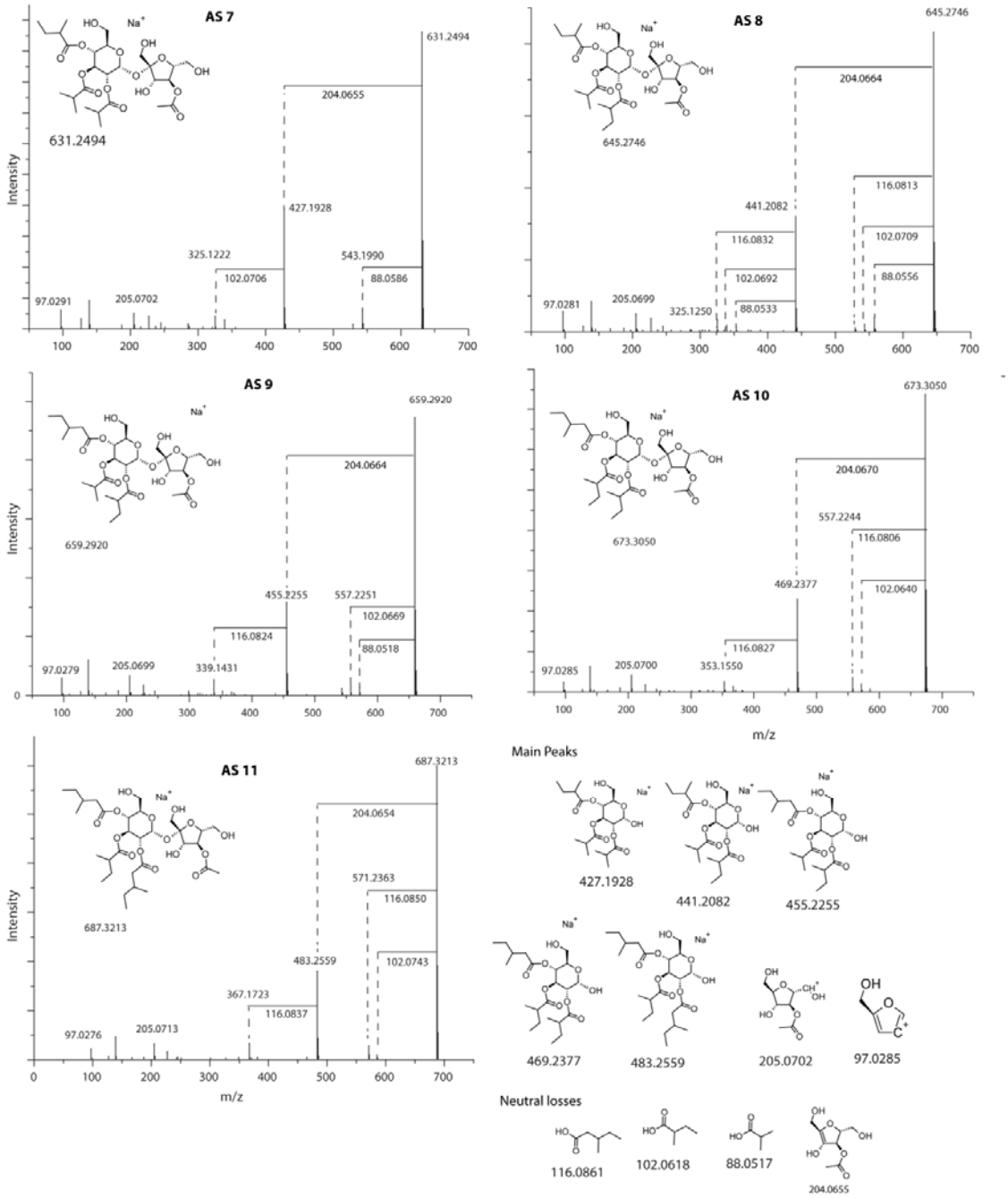

Figure S3: MS^2 spectra of class 3 *O*-acyl sugars and the annotation of the main fragment peaks (Main peaks) and neutral losses. The position of the branched-chain fatty acids could not be verified and may vary.

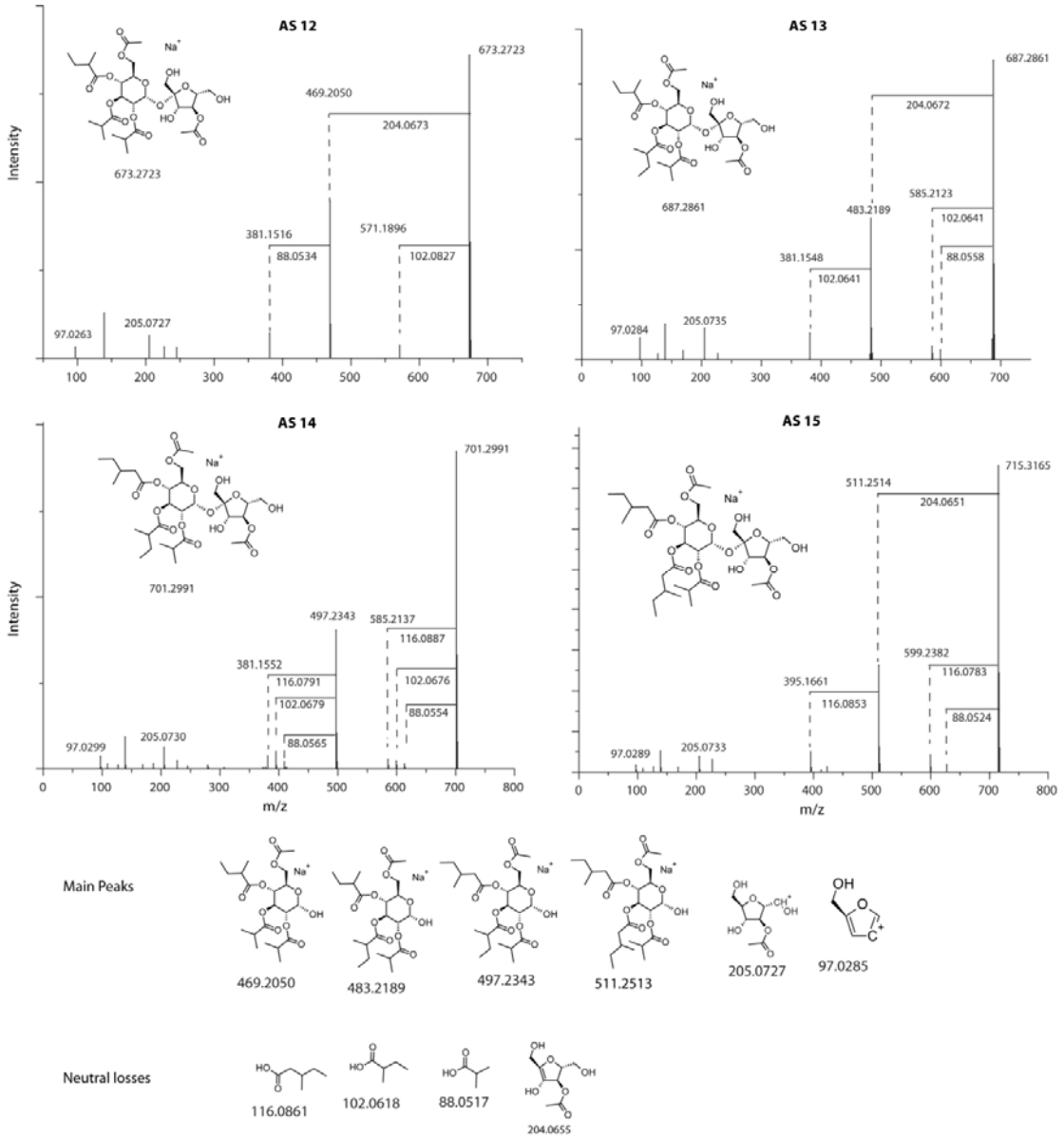

Figure S4: MS^2 spectra of class 4 *O*-acyl sugars and the annotations of the main fragment peaks (Main peaks) and neutral losses. The position of the branched-chain fatty acids could not be verified and may vary.

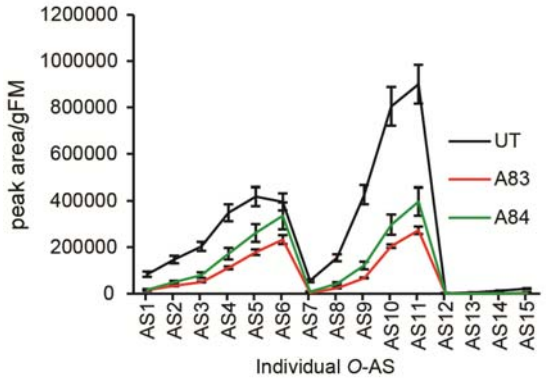

Figure S5. *O*-acyl sugars composition of A83, A84 and UT plants. Peak area per gram fresh mass (peak area/gFM) of each individual *O*-AS revealing the overall reduction of all 15 *O*-AS in A83 and A84 compared to UT.

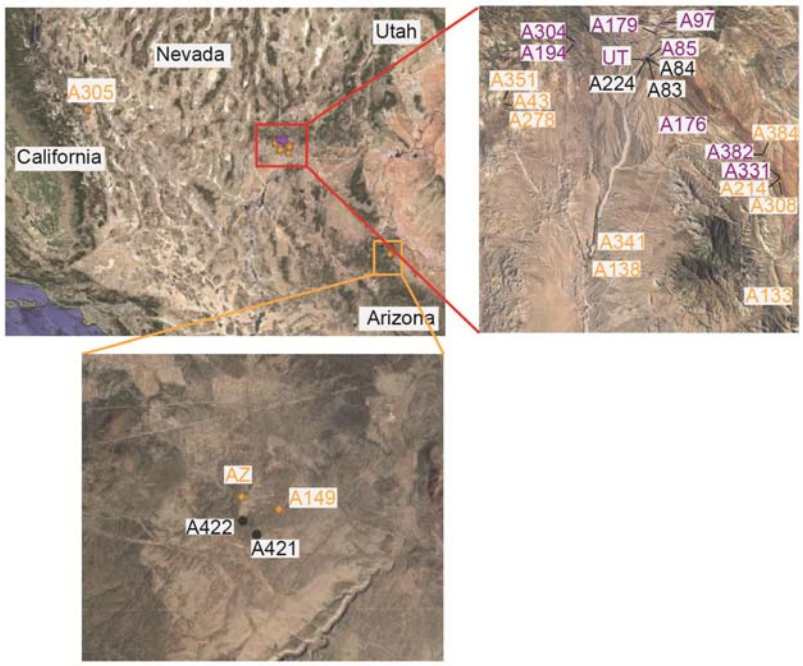

Figure S6. **The location of the 26 accessions collection sites in Utah, Nevada, Arizona, and California**. A close-up for the collection sites in Utah and Arizona are presented. Full GPS coordinates are provided in SI Appendix, Table S1. Colors were given to accessions according to their cluster based on *O*-AS composition (Fig. 2B).

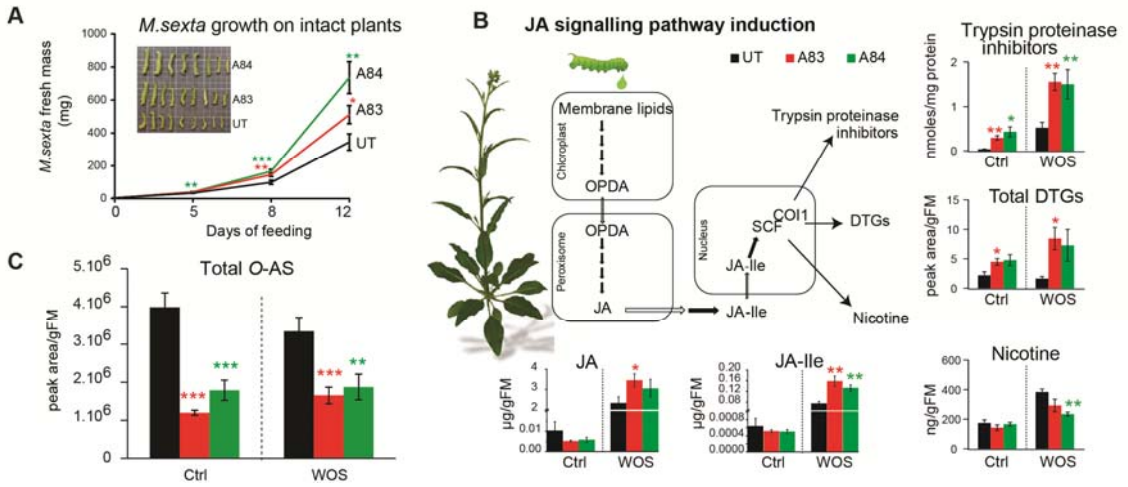

Figure S7. **Two low *O*-AS accessions are not compromised in JA signaling but more susceptible to the specialist herbivore**. **A.** *M. sexta* larvae fed on A83 (red line) and A84 (green line) plants grew faster than those fed on UT plants. The error bars represent standard errors (n=30). **B**. The JA-induced defenses in two low *O*-AS accessions are intact. A simplified herbivore-induced JA signaling and the defensive responses it activates in *N. attenuata* are shown in the middle and five measured traits are shown as bar plots. µg/gFM: µg per gram of fresh mass. Ctrl: control, WOS: wound leaf plus *M. sexta*'s oral secretion. Black bars represent UT while red and green bars represent A83 and A84 plants, respectively. The error bars represent standard error (n= 5- 6). **C**. *O*-AS are not induced after herbivory. In all panels, asterisks indicate significant differences between A83 (red asterisks) or A84 (green asterisks) and UT at a given treatment or a given time point (*t* test, ***: $P \leq 0.001$, **: $P \leq 0.01$,*: $P \leq 0.05$).

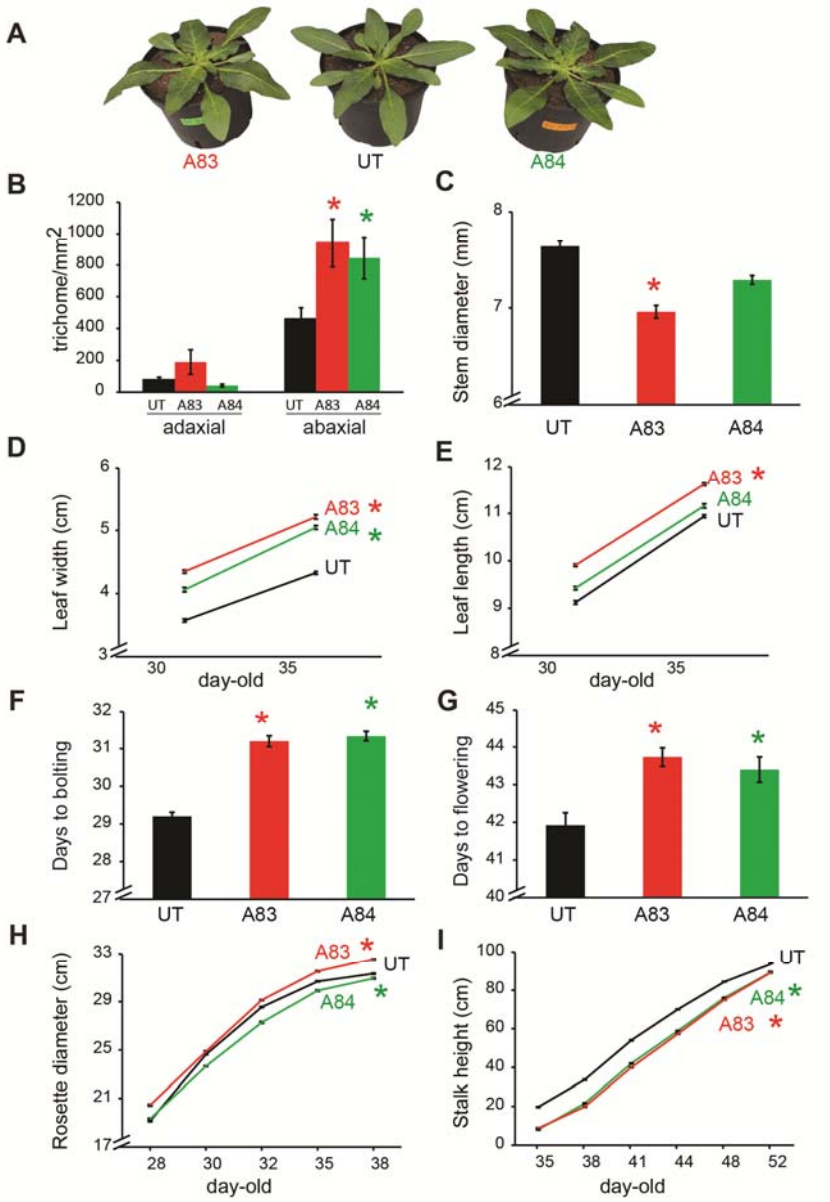

Figure S8. Morphological differences between UT, A83 and A84 plants. **A**. Representative pictures of UT, A83 and A84 plants at the rosette-stage of growth (30 day-old plants). **B**. Trichome density on the leaves of UT, A83 and A84 plants (n=5). Stem diameter (**C**), leaf width (**D**), leaf length (**E**), the number of days to bolting (**F**), the number of days to flowering (**G**), rosette diameter (**H**) and stalk height (**I**) of UT compared to that of A83 and A84. Asterisks indicate significant differences between A83 (red asterisks) or A84 (green asterisks) and UT at a given treatment (*t* test, *: P ≤0.05). Note the breaks in the Y-axis.

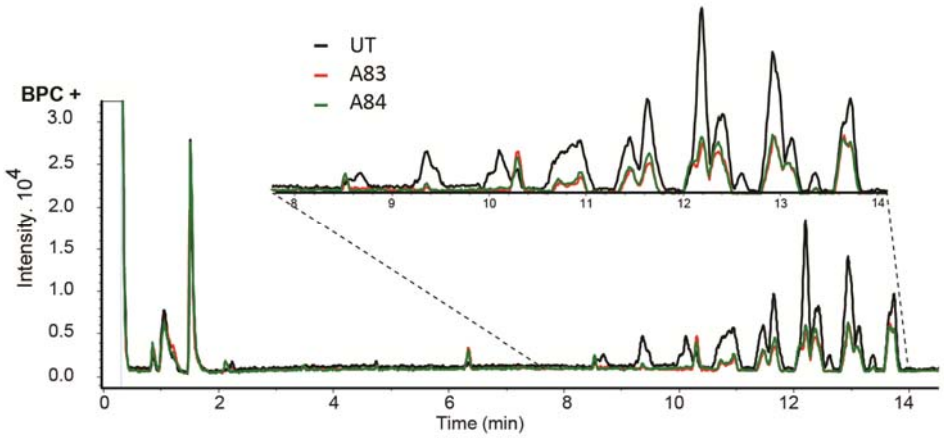

Figure S9. A83 and A84 show less *O*-acyl sugars in the water wash compared to UT. Base peak chromatogram of a positive mode UHPLC/TOF-MS analysis (BPC+) from UT (black line), A83 (red line), A84 (green line) of a 1st water leaf wash.

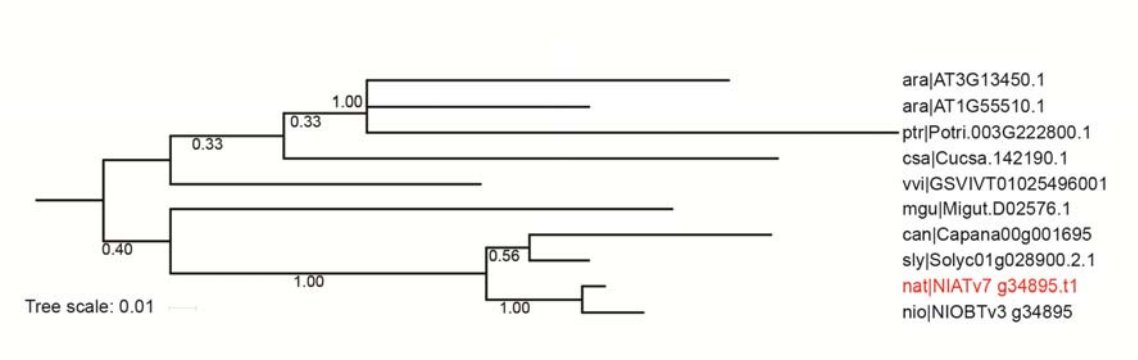

Figure S10. Phylogenetic relationships of genes encoding branched-chain alpha-keto acid dehydrogenase E1 beta subunit among *N. attenuata* and other closely related species. The tree was constructed using the Maximum Likelihood method based on the whole gene sequences using MEGA5 software with General time reversible model. Sequences were aligned using ClustalW algorithm implemented in the MegAlign software. The numbers on the nodes indicate bootstrap scores (500 steps) (Tamura et al., 2010).The numbers on the scale indicates divergence times with relative units. Species names: ara| *Arabidopsis thaliana* (*At*); ptr| *Populus trichocarpa* (*Potri*.); csa| *Cucumis sativus* (*Cucsa*); vvi| *Vitis vinifera* (*Vi*); mgu| *Mimulus guttatus* (Migut); nat| *Nicotiana attenuata* (*NIAT*); nio| *Nicotiana obtusifolia* (*NIOBT*); sly| *Solanum lycopersicum* (*Sl*); can| *Capsicum annuum* (*Capana*)

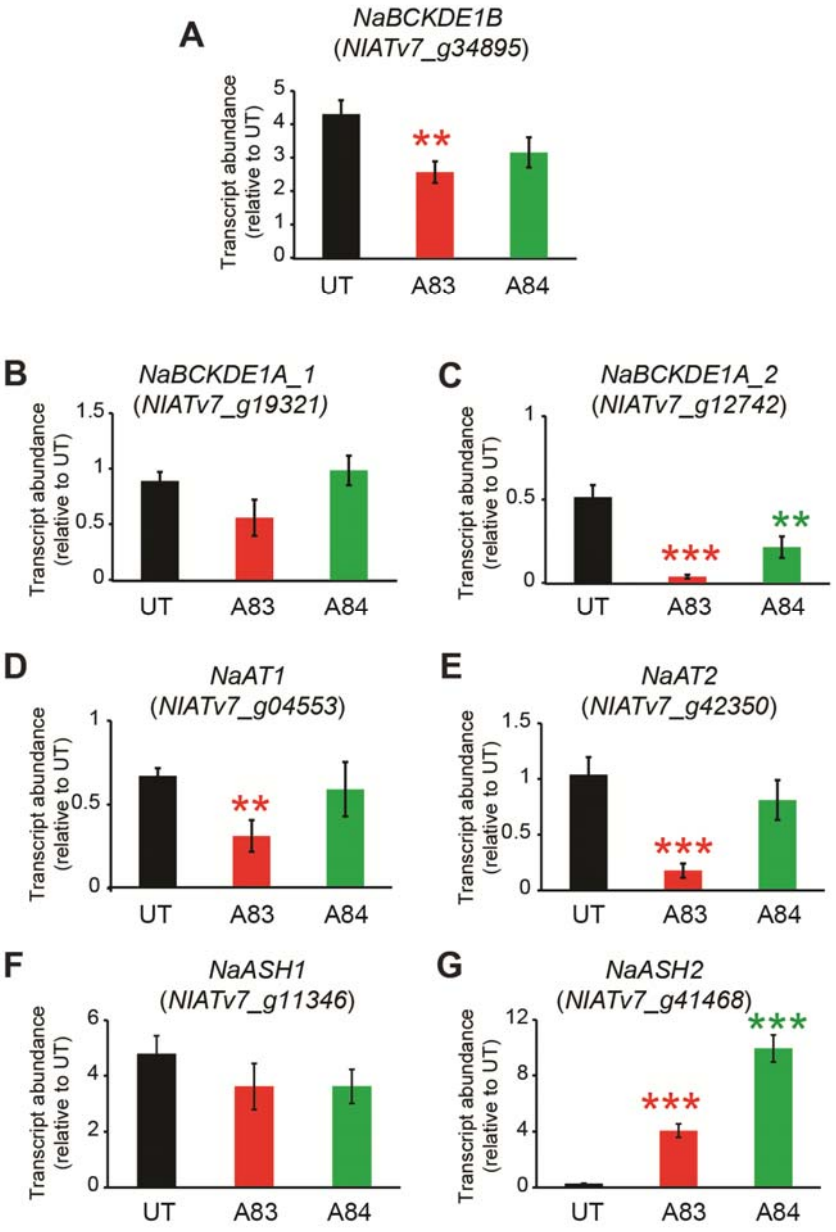

68

69 **Figure S11. Gene expression in trichomes of UT in comparison to A83 and A84**. Relative expression of *N.*
70 *attenuata* genes encoding putative branched-chain alpha-ketoacid dehydrogenase *NaBCKDE1B* (**A**),
71 *NaBCKDE1A* (**B**, **C**), acyltransferases *NaAT1* (**D**), *NaAT2* (**E**), acylsugar acyl hydrolase *NaASH1* (**F**), *NaASH2*
72 (**G**) in trichomes between A83, 84 compared to UT (n=5-6). Relative gene expression was normalized to the
73 expression of the house keeping gene *N. attenuata* actin 7. Asterisks indicate significant differences between
74 A83 (red asterisks) or A84 (green asterisks) and UT at a given treatment (*t* test, ***: $P \leq 0.001$, **: $P \leq 0.01$,*: P
75 ≤ 0.05).

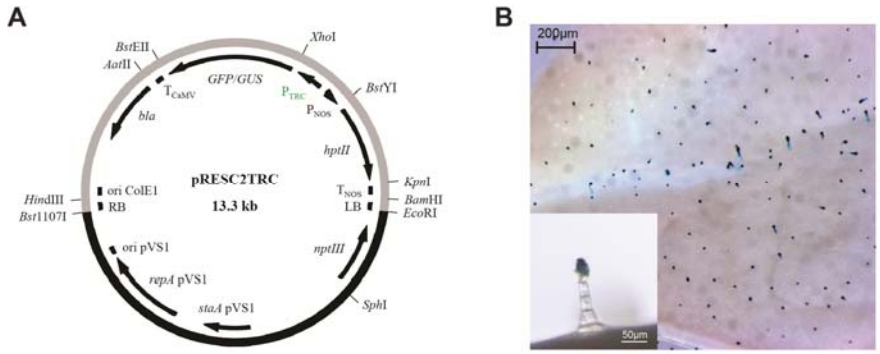

Figure S12. Expression specificity of *S. lycopersicum* trichome specific promoter (SlAT2) in *N. attenuata*. **A**. The pRESC2TRC series binary plant transformation vectors used for expressing SlAT2::GFP/GUS in *N. attenuata*. The1495bp of the trichome-specific promoter from *S. lycopersicum* SlAT2 gene was inserted into pRESC2TRC vector with the hygromycin (*hptII*) resistance gene as a selection marker. Abbreviations: LB/RB, left/right border of T-DNA; PNOS/TNOS, promoter/terminator of the nopaline synthase gene from the Ti plasmid of *Agrobacterium tumefaciens*; PTRC, trichome specific promoter from *Solanum lycopersicum* SlAT2; T35S, 35S terminator from cauliflower mosaic virus; *hptII*, hygromycin phosphotransferase gene from pCAMBIA-1301 (AF234297); *nptII*,amino glycoside phosphotransferase class II; ori, origin of replication. **B**. SlAT2::GUS is expressed in tip cells of both type C and D trichome of *N. attenuata*. Images obtained using a ZEISS stereomicroscope SV 11 with 4x and Axio Zoom.V16 Stereo microscope at 180X magnification.

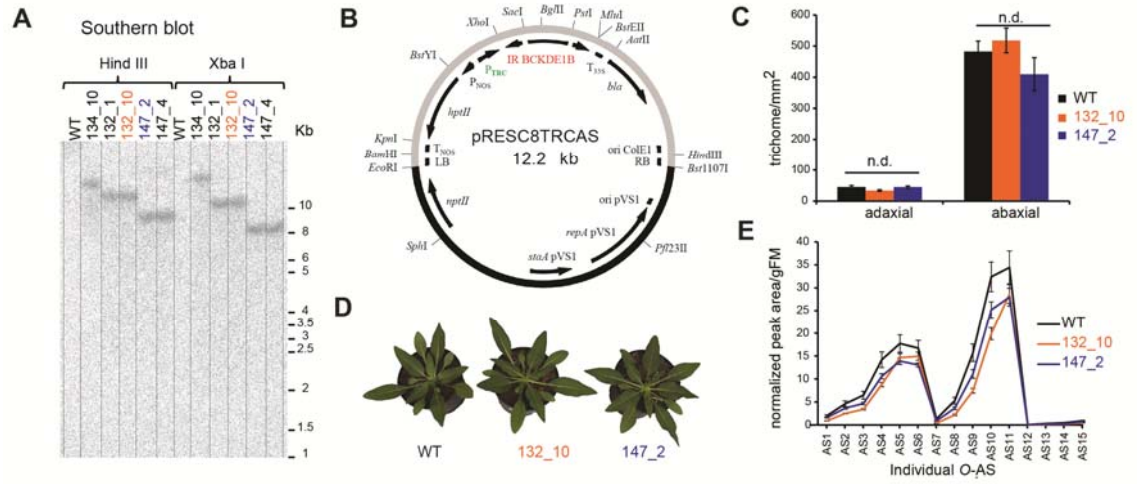

Figure S13. Creating irBCKDE1B transgenic lines using *Agrobacterium*-transformation. **A**. Two *Agrobacterium*-transformed lines irBCKDE1B-132-10 and irBCKDE1B-147-2 were subjected to Southern blot analysis using genomic DNA digested with HindIII and XbaI restriction enzyme and hptII-radiolabeled probe. Both lines showed single insertions of T-DNA fragment into the genome. **B**. The pRESC8TRCAS series binary plant transformation vectors used for silencing BCKDE1B encoding gene (*NIATv7_g34895*).A 351bp of NaBCKDE1B gene was inserted into pRESC8TRCAS vector as an inverted-repeat construct with hptII used as plant selection marker gene. Abbreviations: LB/RB, left/right border of T-DNA; PNOS/TNOS, promoter/terminator of the nopaline synthase gene from the Ti plasmid of *Agrobacterium tumefaciens*; PTRC, trichome specific promoter from *Solanum lycopersicum* SlAT2; T35S, 35S terminator from cauliflower mosaic virus; *hptII*, hygromycin phosphotransferase gene from pCAMBIA-1301 (*AF234297*); i, intron 3 of

Flaveriatrinerviapdk gene for pyruvate, orthophosphate dikinase; *nptII*,amino glycoside phosphotransferase class II; ori, origin of replication. **C**. Trichome density of two independently transformed homozygous irBCKDE1B lines and wild-type (WT) plants (n=5). **D** The similarity of the morphology of two *Agrobacterium*-transformed lines irBCKDE1B-132-10 and irBCKDE1B-147-2 at the rosette-stage of growth. **E**. Individual *O*-AS in 2 irBCKDE1B independent lines. Error bars represent standard error. Asterisks indicate significant differences between WT and individual irBCKDE1B lines (*t* test, ***: P ≤ 0.001, **: P ≤0.01,*: P ≤0.05).

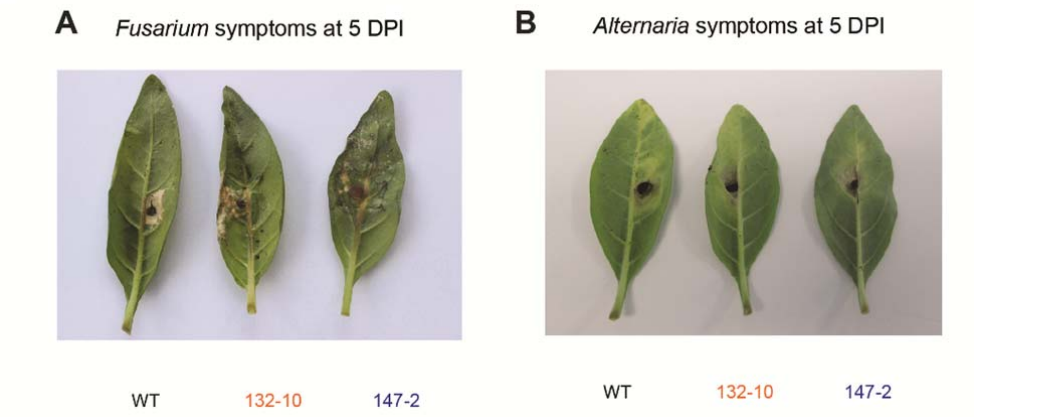

Figure S14. Detached leaf assay on irBCKDE1B transgenic lines. Necrotic lesions caused by *Fusarium* (**A**) and *Alternaria* (**B**) and on detached leaves of WT, 132-10 and 147-2 at 5 days post inoculation (DPI **)**

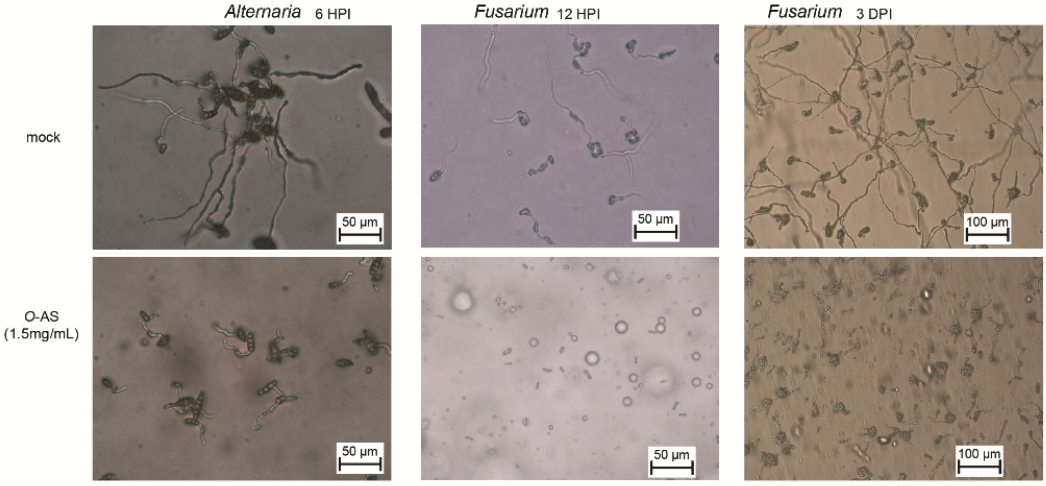

Figure S15. Effect of *O*-acyl sugars on fungal pathogens. Spore germination and hyphal length of *Alternaria* and *Fusarium* fungal on plain agar supplemented with *O*-AS concentrations 1.5 mg/mL in comparison with mock treatment at 6 and 12 h post inoculation (HPI) or 3 days post inoculation (DPI). Pictures were taken under the light microscope Axio Observer.D1 with 400 X magnification.

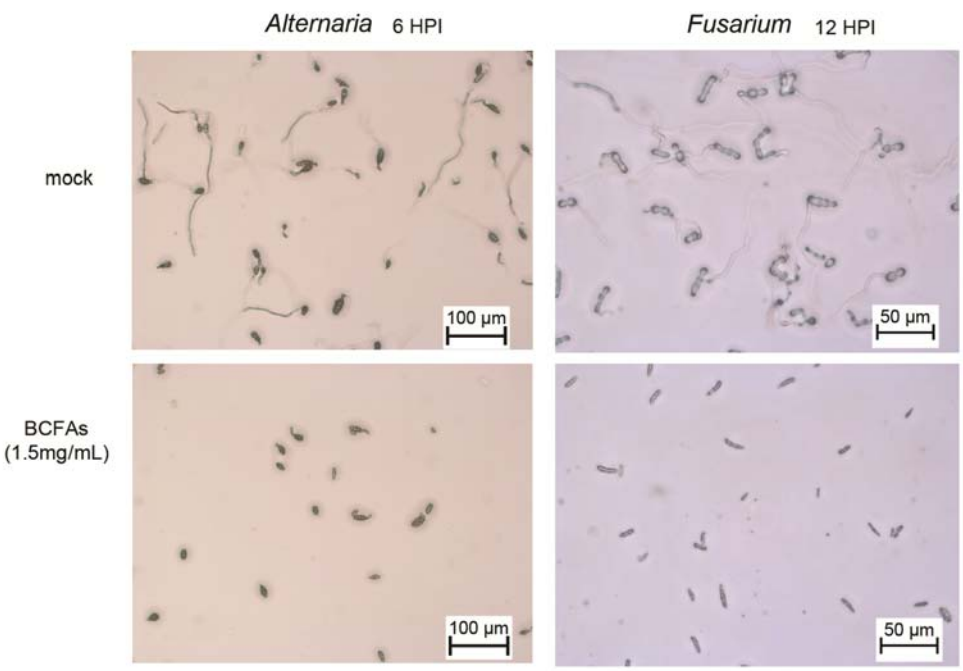

Figure S16. Effect of branched-chain fatty acids (BCFAs) on fungal pathogens. Spore germination and hyphal length of *Alternaria* and *Fusarium* fungal on plain agar supplemented with BCFAs at concentrations of 1.5 mg/mL in comparison with mock treatment at 6 and 12 h post inoculation (HPI). Pictures were taken under the light microscope Axio Observer.D1 with 400 X magnification.

Literature Cited

Tamura K, Peterson D, Peterson N, Stecher G, Nei M, Kumar S. 2011. MEGA5: Molecular evolutionary genetics analysis using maximum likelihood, evolutionary distance, and maximum parsimony methods. Molecular Biology and Evolution 28(10): 2731-2739.

Supplemental Tables

Table S1: GPS coordinates of 26 natural accessions

No. of accession	Accession	Latitude	Longitude
1	A84	37°19'35.48"N	113°57'38.28"W
2	A83	37°19'35.48"N	113°57'38.28"W
3	A422	35°12'44.80"N	111°28'24.80"W
4	A421	35°12'31.10"N	111°28'8.38"W
5	A278	37°16'16.22"N	114° 7'39.67"W
6	A305	37°45'19.61"N	118°35'41.82"W
7	A224	37°19'33.89"N	113°57'54.16"W
8	A138	37° 8'19.58"N	114° 1'35.10"W
9	A351	37°17'9.10"N	114° 7'31.50"W
10	UT	37°19'36.26"N	113°57'53.05"W
11	A133	37° 6'12.50"N	113°49'36.60"W
12	Az	35°13'8.62"N	111°28'26.03"W
13	A308	37°13'5.50"N	113°48'24.25"W
14	A149	35°12'56.07"N	111°27'41.29"W
15	A43	37°17'9.10"N	114° 7'31.50"W
16	A214	37°13'15.83"N	113°48'20.86"W
17	A384	37°14'27.05"N	113°49'36.71"W
18	A304	37°20'22.52"N	114° 2'40.86"W
19	A341	37° 9'45.30"N	114° 0'58.52"W
20	A331	37°13'15.83"N	113°48'20.86"W
21	A194	37°20'22.52"N	114° 2'40.86"W
22	A97	37°21'35.24"N	113°56'38.68"W
23	A382	37°14'27.05"N	113°49'36.71"W
24	A176	37°16'38.65"N	113°53'35.18"W
25	A179	37°21'1.04"N	113°57'5.17"W
26	A85	37°19'35.48"N	113°57'38.28"W

Table S2. The list of m/z and retention times (RT) used to identify and measure *O*-acyl sugars (*O*-AS). *O*-AS annotation was done as described by Kim et al. (2012) which includes sucrose backbone (S for sucrose), the number of acyl chains, the total number of carbons for acyl chains and the expected length of each acyl chain. For instance, S3:13(4,5,4): acyl sucrose with 3 acyl chains of 4, 5 and 4 carbons, so in total 13 carbons.

***O*-acyl sugars**	***O*-AS annotation**	**m/z**	**m/z width**	**RT(min)**	**RT width**
AS1	S3:13(4,5,4)	589.24	0.05	8.6	0.5
AS2	S3:14 (5,4,5)	603.26	0.05	9.4	0.5
AS3	S3:15 (5,5,5)	617.27	0.05	10.1	0.5
AS4	S3:16 (6,5,5)	631.29	0.01	10.9	0.5
AS5	S3:17 (6,5,6)	645.31	0.01	11.7	0.5
AS6	S3:18 (6,6,6)	659.32	0.01	12.3	0.5
AS7	S4:15 (2,4,4,5)	631.25	0.05	9.9	0.5
AS8	S4:16 (2,5,4,5)	645.27	0.01	10.7	0.5
AS9	S4:17 (2,5,4,6)	659.29	0.01	11.3	0.5
AS10	S4:18 (2,5,5,6)	673.3	0.01	12	0.5
AS11	S4:19 (2,6,5,6)	687.32	0.01	12.9	0.5
AS12	S5:17 (2,4,4,5)	673.27	0.01	11.1	0.5
AS13	S5:18 (2,4,5,5,2)	687.28	0.01	11.8	0.5
AS14	S5:19 (2,4,5,6,2)	701.29	0.01	12.6	0.5
AS15	S5:20 (2,4,6,6,2)	715.31	0.01	13.4	0.5

Table S3: Branched-chain fatty acids (BCFAs) compositions of *N. attenuata O*-acyl sugars (*O*-AS). Retention times (RT) and indices (RI) of authentic standards are compared to those found in the extract of saponified *O*-AS. The most abundant BCFAs are highlighted (bold).

		RT	**RI**	**RT**	**RI**
	Acid	Single Standards		extracthydrolysis	
1	aceticacid	19.386	1456	19.319	1453
2	propionicacid	21.538	1543	21.603	1546
3	**2-methyl propanoicacid**	22.281	1574	22.124	1567
4	**2-methy butanoicacid**	24.679	1678	24.501	1670
5	**3-methyl butanoicacid**	24.678	1678	24.501	1670
6	**3-methyl pentanoicacid**	27.393	1802	27.265	1796
7	**4-methyl pentanoicacid**	27.601	1813	27.46	1806
8	hexanoicacid	28.536	1859	28.426	1853

Table S4: MS^2-spectral data showing the annotation of class 2 *O*-acyl sugars elemental formulas, their calculated monoisotopic mass, the elemental formula of fragment ions, and their annotations, intensity and m/z values compared to the calculated m/z values.

ID	Monoisotopic mass El Formula	Elemental Formula Fragments	Annotation	Intensity	m/z Fragment	m/z Calc	Δppm
AS1	566.2926 $C_{25}H_{42}O_{14}$	$C_{25}H_{42}O_{14}Na^+$	$[M+Na]^+$	14.68	589.2477	589.2467	1
		$C_{19}H_{32}O_9Na^+$	$[(M -C_6H_{10}O_5)+Na]^+$	100.00	427.1935	427.1938	0.3
		$C_{15}H_{24}O_7Na^+$	$[(M -C_6H_{10}O_5 - C_4H_8O_2)+Na]^+$	4.36	339.1383	339.1414	3.1
		$C_{14}H_{22}O_7Na^+$	$[(M -C_6H_{10}O_5 - C_5H_{10}O_2)+Na]^+$	5.88	325.1317	325.1257	6
		$C_6H_{10}O_5Na^+$	$[(M -C_{19}H_{32}O_9)+Na]^+$	3.33	185.0404	185.042	1.6
AS2	580.2731 $C_{26}H_{44}O_{14}$	$C_{26}H_{44}O_{14}Na^+$	$[M+Na]^+$	100.00	603.2663	603.2623	4
		$C_{20}H_{34}O_9Na^+$	$[(M -C_6H_{10}O_5)+Na]^+$	33.88	441.2048	441.2095	4.7
		$C_{15}H_{24}O_7Na^+$	$[(M -C_6H_{10}O_5 - C_4H_8O_2)+Na]^+$	7.52	353.1583	353.1571	1.2
		$C_{15}H_{24}O_7Na^+$	$[(M -C_6H_{10}O_5 - C_5H_{10}O_2)+Na]^+$	6.58	339.1448	339.1414	3.4
		$C_6H_{10}O_5Na^+$	$[(M -C_{20}H_{34}O_9)+Na]^+$	4.36	185.0404	185.042	1.6
AS3	594.2887 $C_{27}H_{46}O_{14}$	$C_{27}H_{46}O_{14}Na^+$	$[M+Na]^+$	16.82	617.2756	617.2779	2.3
		$C_{21}H_{36}O_9Na^+$	$[(M -C_6H_{10}O_5)+Na]^+$	100.00	455.2249	455.2251	0.2
		$C_{17}H_{28}O_7Na^+$	$[(M -C_6H_{10}O_5 - C_4H_8O_2)+Na]^+$	1.83	367.1745	367.1727	1.8
		$C_{16}H_{26}O_7Na^+$	$[(M -C_6H_{10}O_5 - C_5H_{10}O_2)+Na]^+$	6.13	353.1538	353.157	3.2
		$C_{15}H_{24}O_7Na^+$	$[(M -C_6H_{10}O_5 - C_6H_{12}O_2)+Na]^+$	4.30	339.1365	339.1414	4.9
		$C_6H_{10}O_5Na^+$	$[(M -C_{21}H_{36}O_9)+Na]^+$	2.88	185.0406	185.042	1.4
AS4	608.3044 $C_{28}H_{48}O_{14}$	$C_{28}H_{48}O_{14}Na^+$	$[M+Na]^+$	18.98	631.2962	631.2926	3.6
		$C_{22}H_{38}O_9Na^+$	$[(M -C_6H_{10}O_5)+Na]^+$	100.00	469.2403	469.2408	0.5
		$C_{17}H_{28}O_7Na^+$	$[(M -C_6H_{10}O_5 - C_5H_{10}O_2)+Na]^+$	2.54	367.1625	367.1727	10.2
		$C_{16}H_{26}O_7Na^+$	$[(M -C_6H_{10}O_5 - C_6H_{12}O_2)+Na]^+$	7.66	353.1575	353.157	0.5
		$C_6H_{10}O_5Na^+$	$[(M -C_{22}H_{38}O_9)+Na]^+$	2.71	185.0419	185.042	0.1
AS5	622.3201 $C_{29}H_{50}O_{14}$	$C_{29}H_{50}O_{14}Na^+$	$[M+Na]^+$	20.23	645.3117	645.3093	2.4
		$C_{23}H_{40}O_9Na^+$	$[(M -C_6H_{10}O_5)+Na]^+$	100.00	483.2553	483.2564	1.1
		$C_{18}H_{30}O_7Na^+$	$[(M -C_6H_{10}O_5 - C_5H_{10}O_2)+Na]^+$	2.33	381.1848	381.1883	3.5
		$C_{17}H_{28}O_7Na^+$	$[(M -C_6H_{10}O_5 - C_6H_{12}O_2)+Na]^+$	9.52	367.1711	367.1727	1.6
		$C_6H_{10}O_5Na^+$	$[(M -C_{23}H_{40}O_9)+Na]^+$	3.42	185.0412	185.042	0.8
AS6	636.3249 $C_{30}H_{52}O_{14}$	$C_{30}H_{52}O_{14}Na^+$	$[M+Na]^+$	25.23	659.324	659.3249	0.9
		$C_{24}H_{42}O_9Na^+$	$[(M -C_6H_{10}O_5)+Na]^+$	100.00	497.2725	497.2721	0.4
		$C_{18}H_{30}O_7Na^+$	$[(M -C_6H_{10}O_5 - C_6H_{12}O_2)+Na]^+$	9.24	381.1893	381.1883	1
		$C_6H_{10}O_5Na^+$	$[(M -C_{24}H_{42}O_9)+Na]^+$	2.54	185.0408	185.042	1.2

Table S5: MS^2-spectral data showing the annotations of class 3 *O*-acyl sugars elemental formulas, their calculated monoisotopic mass, the elemental formula of fragment ions, their annotations, intensity and m/z values compared to the calculated m/z values.

ID	Monoisotopic mass El Formula	Elemental Formula Fragments	Annotation	Intensity	m/z Fragment	m/z Calc	Δppm
AS7	608.2680 $C_{27}H_{44}O_{15}$	$C_{27}H_{44}O_{15}Na^+$	$[M+Na]^+$	100.00	631.2554	631.2572	1.8
		$C_{23}H_{36}O_{13}Na^+$	$[(M - C_4H_8O_2)+Na]^+$	5.99	543.199	543.2048	5.8
		$C_{19}H_{32}O_9Na^+$	$[(M -C_8H_{12}O_6)+Na]^+$	40.35	427.1928	427.1939	1.1
		$C_{14}H_{22}O_7Na^+$	$[(M -C_8H_{12}O_6 - C_5H_{10}O_2)+Na]^+$	4.27	325.1222	325.1258	3.6
		$C_8H_{13}O_6^+$	$[M -C_{19}H_{31}O_9Na]^+$	5.32	205.0702	205.0706	0.4
		$C_5H_5O_2^+$	$[C_8H_{13}O_6 - C_2H_4O_2 - HCHO - H_2O]^+$	6.32	97.0291	97.0285	0.6
AS8	622.2837 $C_{28}H_{46}O_{15}$	$C_{28}H_{46}O_{15}Na^+$	$[M+Na]^+$	100.00	645.2746	645.2729	1.7
		$C_{24}H_{38}O_{13}Na^+$	$[(M - C_4H_8O_2)+Na]^+$	4.83	557.219	557.2204	1.4
		$C_{23}H_{36}O_{13}Na^+$	$[(M - C_5H_{10}O_2)+Na]^+$	2.55	543.2058	543.2048	1
		$C_{22}H_{34}O_{13}Na^+$	$[(M- C_6H_{12}O_2)+Na]^+$	1.48	529.1925	529.1891	3.4
		$C_{20}H_{34}O_9Na^+$	$[(M -C_8H_{12}O_6)+Na]^+$	38.54	441.2082	441.2095	1.3
		$C_{16}H_{26}O_7Na^+$	$[(M -C_8H_{12}O_6 - C_4H_8O_2)+Na]^+$	1.57	353.1538	353.157	3.2
		$C_{15}H_{24}O_7Na^+$	$[(M -C_8H_{12}O_6 - C_5H_{10}O_2)+Na]^+$	2.22	339.1365	339.1414	4.9
		$C_{14}H_{22}O_7Na^+$	$[(M -C_8H_{12}O_6 - C_6H_{12}O_2)+Na]^+$	4.11	325.125	325.1258	0.8
		$C_8H_{13}O_6^+$	$[M -C_{20}H_{33}O_9Na]^+$	6.09	205.0699	205.0706	0.7
		$C_5H_5O_2^+$	$[C_8H_{13}O_6 - C_2H_4O_2 - HCHO - H_2O]^+$	6.79	97.0281	97.0285	0.4
AS9	636.2993 $C_{29}H_{48}O_{15}$	$C_{29}H_{48}O_{15}Na^+$	$[M+Na]^+$	100.00	659.292	659.2885	3.5
		$C_{25}H_{40}O_{13}Na^+$	$[(M - C_4H_8O_2)+Na]^+$	2.92	571.2342	571.2361	1.9
		$C_{24}H_{38}O_{13}Na^+$	$[(M - C_5H_{10}O_2)+Na]^+$	3.64	557.2251	557.2204	4.7
		$C_{23}H_{36}O_{13}Na^+$	$[(M- C_6H_{12}O_2)+Na]^+$	2.38	543.2059	543.2048	1.1
		$C_{21}H_{36}O_9Na^+$	$[(M -C_8H_{12}O_6)+Na]^+$	33.45	455.2255	455.2251	0.4
		$C_{17}H_{28}O_7Na^+$	$[(M -C_8H_{12}O_6 - C_4H_8O_2)+Na]^+$	1.14	367.1748	367.1727	2.1
		$C_{16}H_{26}O_7Na^+$	$[(M -C_8H_{12}O_6 - C_5H_{10}O_2)+Na]^+$	1.41	353.1542	353.157	2.8
		$C_{15}H_{24}O_7Na^+$	$[(M -C_8H_{12}O_6 - C_6H_{12}O_2)+Na]^+$	5.64	339.1431	339.1414	1.7
		$C_8H_{13}O_6^+$	$[M -C_{21}H_{35}O_9Na]^+$	7.08	205.0699	205.0706	0.7
		$C_5H_5O_2^+$	$[C_8H_{13}O_6 - C_2H_4O_2 - HCHO - H_2O]^+$	6.08	97.0279	97.0285	0.6

Table S5 continued:

ID	Monoisotopic mass El Formula	Elemental Formula Fragments	Annotation	Intensity	m/z Fragment	m/z Calc	Δppm
AS10	650.315 $C_{30}H_{50}O_{15}$	$C_{30}H_{50}O_{15}Na^+$	$[M+Na]^+$	100.00	673.305	673.3041	0.9
		$C_{25}H_{40}O_{13}Na^+$	$[(M - C_5H_{10}O_2)+Na]^+$	2.72	571.2365	571.2361	0.4
		$C_{24}H_{38}O_{13}Na^+$	$[(M- C_6H_{12}O_2)+Na]^+$	4.80	557.2244	557.2204	4
		$C_{22}H_{38}O_9Na^+$	$[(M -C_8H_{12}O_6)+Na]^+$	31.03	469.2377	469.2408	3.1
		$C_{17}H_{28}O_7Na^+$	$[(M -C_8H_{12}O_6 - C_5H_{10}O_2)+Na]^+$	1.95	367.1767	367.1727	4
		$C_{16}H_{26}O_7Na^+$	$[(M -C_8H_{12}O_6 - C_6H_{12}O_2)+Na]^+$	3.46	353.155	353.157	2
		$C_8H_{13}O_6^+$	$[M -C_{22}H_{37}O_9Na]^+$	5.67	205.07	205.0706	0.6
		$C_5H_5O_2^+$	$[C_8H_{13}O_6 - C_2H_4O_2 - HCHO - H_2O]^+$	3.36	97.0276	97.0285	0.9
AS11	664.3306 $C_{31}H_{52}O_{15}$	$C_{31}H_{52}O_{15}Na^+$	$[M+Na]^+$	100.00	687.3213	687.3198	1.5
		$C_{26}H_{42}O_{13}Na^+$	$[(M - C_5H_{10}O_2)+Na]^+$	1.69	585.2495	585.2517	2.2
		$C_{25}H_{40}O_{13}Na^+$	$[(M- C_6H_{12}O_2)+Na]^+$	4.84	571.2363	571.2361	0.2
		$C_{23}H_{40}O_9Na^+$	$[(M -C_8H_{12}O_6)+Na]^+$	30.06	483.2559	483.2565	0.6
		$C_{17}H_{28}O_7Na^+$	$[(M -C_8H_{12}O_6 - C_6H_{12}O_2)+Na]^+$	5.62	367.1723	367.1727	0.4
		$C_8H_{13}O_6^+$	$[M -C_{23}H_{39}O_9Na]^+$	5.41	205.0713	205.0706	0.7
		$C_5H_5O_2^+$	$[C_8H_{13}O_6 - C_2H_4O_2 - HCHO - H_2O]^+$	3.72	97.0285	97.0285	0

Table S6: MS^2-spectral data showing the annotations of class 4 *O*-acyl sugars elemental formulas, their calculated monoisotopic mass, the elemental formula of fragment ions, and their annotations, intensity and m/z values compared to the calculated m/z values.

ID	Monoisotopic mass El Formula	Elemental Formula Fragments	Annotation	Intensity	Fragment Mass	Calc	Δppm
AS 12	650.2786 $C_{29}H_{46}O_{16}$	$C_{29}H_{46}O_{16}Na^+$	$[M+Na]^+$	100.00	673.2723	673.2678	4.5
		$C_{25}H_{38}O_{14}Na^+$	$[(M - C_4H_8O_2)+Na]^+$	3.31	585.2072	585.2153	8.1
		$C_{24}H_{36}O_{14}Na^+$	$[(M - C_5H_{10}O_2)+Na]^+$	4.42	571.1896	571.1997	10.1
		$C_{21}H_{34}O_{10}Na^+$	$[(M -C_8H_{12}O_6)+Na]^+$	51.73	469.205	469.2044	0.6
		$C_{17}H_{26}O_8Na^+$	$[(M -C_8H_{12}O_6 - C_4H_8O_2)+Na]^+$	8.37	381.1516	381.1519	0.3
		$C_8H_{13}O_6^+$	$[M -C_{21}H_{33}O_{10}Na]^+$	7.53	205.0727	205.0706	2.1
		$C_5H_5O_2^+$	$[C_8H_{13}O_6 - C_2H_4O_2 - HCHO - H_2O]^+$	3.72	97.0263	97.0285	2.2
AS 13	664.2942 $C_{30}H_{48}O_{16}$	$C_{30}H_{48}O_{16}Na^+$	$[M+Na]^+$	100.00	687.2861	687.2835	2.6
		$C_{26}H_{40}O_{14}Na^+$	$[(M - C_4H_8O_2)+Na]^+$	3.36	599.2303	599.231	0.7
		$C_{25}H_{38}O_{14}Na^+$	$[(M - C_5H_{10}O_2)+Na]^+$	4.52	585.2123	585.2153	3
		$C_{22}H_{36}O_{10}Na^+$	$[(M -C_8H_{12}O_6)+Na]^+$	47.27	483.2189	483.2201	1.2
		$C_{17}H_{26}O_8Na^+$	$[(M -C_8H_{12}O_6 - C_5H_{10}O_2)+Na]^+$	8.99	381.1548	381.1519	2.9
		$C_8H_{13}O_6^+$	$[M -C_{22}H_{35}O_{10}Na]^+$	10.54	205.0735	205.0706	2.9
		$C_5H_5O_2^+$	$[C_8H_{13}O_6 - C_2H_4O_2 - HCHO - H_2O]^+$	7.30	97.0284	97.0285	0.1
AS 14	678.3098 $C_{31}H_{50}O_{16}$	$C_{31}H_{50}O_{16}Na^+$	$[M+Na]^+$	100.00	701.2973	701.2991	1.8
		$C_{27}H_{42}O_{14}Na^+$	$[(M - C_4H_8O_2)+Na]^+$	1.58	613.2455	613.2467	1.2
		$C_{26}H_{40}O_{14}Na^+$	$[(M - C_5H_{10}O_2)+Na]^+$	2.58	599.2348	599.231	3.8
		$C_{25}H_{38}O_{14}Na^+$	$[(M- C_6H_{12}O_2)+Na]^+$	2.90	585.2137	585.2153	1.6
		$C_{23}H_{38}O_{10}Na^+$	$[(M -C_8H_{12}O_6)+Na]^+$	43.62	497.2343	497.2357	1.4
		$C_{19}H_{30}O_8Na^+$	$[(M -C_8H_{12}O_6 - C_4H_8O_2)+Na]^+$	2.15	409.1778	409.1832	5.4
		$C_{18}H_{28}O_8Na^+$	$[(M -C_8H_{12}O_6 - C_5H_{10}O_2)+Na]^+$	5.48	395.1664	395.1676	1.2
		$C_{17}H_{26}O_8Na^+$	$[(M -C_8H_{12}O_6 - C_6H_{12}O_2)+Na]^+$	4.11	381.1552	381.152	3.2
		$C_8H_{13}O_6^+$	$[M -C_{23}H_{37}O_{10}Na]^+$	6.83	205.0703	205.0706	0.3
		$C_5H_5O_2^+$	$[C_8H_{13}O_6 - C_2H_4O_2 - HCHO - H_2O]^+$	3.96	97.0299	97.0285	1.4
AS 15	692.3225 $C_{32}H_{52}O_{16}$	$C_{32}H_{52}O_{16}Na^+$	$[M+Na]^+$	100.00	715.3165	715.3148	1.7
		$C_{28}H_{44}O_{14}Na^+$	$[(M - C_4H_8O_2)+Na]^+$	2.46	627.2641	627.2623	1.8
		$C_{26}H_{40}O_{14}Na^+$	$[(M- C_6H_{12}O_2)+Na]^+$	5.74	599.2382	599.231	7.2
		$C_{24}H_{40}O_{10}Na^+$	$[(M -C_8H_{12}O_6)+Na]^+$	34.86	511.2514	511.2513	0.1
		$C_{18}H_{28}O_8Na^+$	$[(M -C_8H_{12}O_6 - C_6H_{12}O_2)+Na]^+$	6.68	395.1661	395.1676	1.5
		$C_8H_{13}O_6^+$	$[M -C_{24}H_{39}O_{10}Na]^+$	5.07	205.0733	205.0706	2.7
		$C_5H_5O_2^+$	$[C_8H_{13}O_6 - C_2H_4O_2 - HCHO - H_2O]^+$	2.24	97.0289	97.0285	0.4

Table S7: The concentration of each branched-chain fatty acids (BCFAs) released from *Manduca sexta*'s frass and bodies as described by Weinhold and Baldwin (2011) and in the reconstructed mixture for the artificial diet and spore germination medium.

	2-methyl butanoic acid	3-methyl butanoic acid	3-methyl pentanoic acid	4-methyl pentanoic acid	Total 4 BCFAs
ng/g frass within 2h	199.6	660.12	5110.2	248.72	6218.64
% in frass within 2h	3.2	10.6	82.2	4.0	
ng/ 3rd instar caterpillar within 2h	44.06	212.32	1210.57	37.17	1504.12
% in 3rd instar caterpillar within 2h	2.9	14.1	80.5	2.5	
mg/g diet	0.04	0.13	0.99	0.05	1.2
% in diet	3.2	10.6	82.2	4.0	
mg/mL medium	0.1	0.32	2.47	0.12	3
% in medium	3.2	10.6	82.2	4.0	

Literature Cited

Brockmöller T, Ling Z, Li D, Gaquerel E, Baldwin IT, Xu S. 2017. *Nicotiana attenuata* Data Hub (NaDH): an integrative platform for exploring genomic, transcriptomic and metabolomic data in wild tobacco. BMC Genomics 18(1): 79.

Kim J, Kang K, Gonzales-Vigil E, Shi F, Jones AD, Barry CS, Last RL (2012) Striking natural diversity in glandular trichome acylsugar composition is shaped by variation at the acyltransferase2 locus in the wild tomato *Solanum habrochaites*. Plant Physiology 160: 1854-1870

Weinhold A, Baldwin IT (2011) Trichome derived *O*-acyl sugars are a first meal for caterpillars that tags them for predation. Proceedings of the National Academy of Sciences of the United States of America 108: 7855-7859

Supplemental Methods

O-AS isolation and characterization

To isolate *O*-AS from *N. attenuata* plants, we used a protocol similar to that of Van Dam and Hare (1998). All plant parts except the flowers were harvested. The stem was cut into small pieces (approx. 10cm). Around 1 kg of tissue was combined in a 5 L glass beaker (Schott) and soaked in 3 L of chloroform for 1h of stirring. Afterwards, the plant tissue was removed and the solvent was dried over sodium sulfate (anhydrous Sigma-Aldrich). The chloroform was removed in a rotary evaporator and the residue was resolved in acetonitrile (ACN) (VWR International) and sonicated. The ACN phase was partitioned 3 times against n-hexane (VWR International) (ACN: n-Hexane 1:2). The hexane phase was discarded and the ACN was removed in a rotary evaporator. The residue was solved in dichloromethane (DCM) (VWR) and partitioned 3 times against 1N tartaric acid (Sigma-Aldrich) 2 times against distilled water. Afterward, the DCM was removed and the glue-like, brownish yellow residue was kept under argon at 4°C until further use for bioassay and for MS^2 experiment. A small portion was dissolved in 40% methanol and analyzed by ultra-high performance liquid chromatography/ time-of-flight mass spectrometry (UHPLC/TOF-MS) to verify the extraction.

To fragment the *O*-AS for MS^2 experiment, extracted *O*-AS was dissolved in acetonitrile to a concentration of 1mg/mL. We used an Agilent 1100 HPLC system equipped with a DAD detector. Separation was achieved on a preparative Luna 5n C18 column (250 x 10 mm, 5µm, Phenomenex) connected to a Luna 5n C-18 guard column (50 x 10 mm, 5 µm) with a mixture of deionized water (0.1 % (v/v) formic acid + 0.1% (v/v) ammonia) (solvent A) and methanol (solvent B) at a flow rate of 3 mL/min. We used an isocratic gradient with 80 % of solvent B for 20 min and then increased to 95% of solvent B in 5 min. The post-run time was 7 min. We collected fractions with a Foxy fraction collector (Isco) in 20 mL glass reaction tubes (Schott). 40 fractions of 30 s were cut starting 5 min. after injection. The fractions were transferred to scintillation vials and the solvent was evaporated in a vacuum centrifuge (Eppendorf). The single fractions were then analyzed for their content by injection into an UHPLC/TOF-MS system (BrukerDaltonik, Bremen, Germany) with conditions described in Weinhold and Baldwin (2011).

For MS^2 experiments, 1µL of each fraction was separated using a Dionex RSLC system (Dionex, Sunnyvale, USA) with a Dionex Acclaim RSLC 120 C-18 column (150 x 2.1 mm, 2.2 µm). The following binary gradient was applied: 0 to 1 min isocratic 90% A (deionized water, 0.1% (v/v) acetonitrile (Baker, HPLC grade), and 0.05% formic acid), 10% B (acetonitrile and 0.05%formic acid); 1 to 9 min linear gradient to 80% B; isocratic for 2 min. The flow rate was 400 µL/min. MS detection was carried out with an ultra-high performance liquid chromatography/quadrupole time-of-flight mass spectrometry (UHPLC/Q-TOF-MS) (BrukerDaltonik, Bremen, Germany) operated in positive electrospray mode. Typical instrument settings were as follows: capillary voltage, 4500 V; dry gas temperature, 180 °C; dry gas flow, 10 L/min. Ions were detected from m/z 50 to 1400 at a repetition rate of 1 Hz. The instrument was operated in autoMS/MS mode at various CID voltages from 5 to 75 eV for sodium adducts. Mass calibration was performed using sodium formate clusters (10 mM solution of NaOH in 50/50% v/v isopropanol/water containing 0.2% formic acid). Elemental formula and mass were calculated with the ACD/Labs 12 ChemSketch calculating tool (ACD/Labs, Frankfurt, Germany).

Analysis of *O*-AS acid composition

One mg of an *O*-AS extract, obtained as described above, was saponified by adding 1 mL of a 0.2 M aqueous potassium hydroxide solution (Sigma-Aldrich). The solution was sonicated and kept in a sealed vial for 24 h. The mixture was neutralized by adding 1 mL of a 0.2 M hydrochloric acid solution and then partitioned against 1.5 mL dichloromethane (VWR). One µL of the dichloromethane phase was then injected into a Varian 3800 gas chromatograph equipped with a ZB-Wax-plus column (30m x 0.25mm x 0.25µm, Restek) and a flame ionization detector (GC-FID) (Agilent). The injector temperature was set to 230°C and the flow was 1 mL/min (constant flow). The oven was kept at 40°C for 5 min, then heated to 185°C at a rate of 5°C/min and finally with a rate of 30°C/min to 250 °C. The FID was operated at 250°C with 25 mL/min make up gas flow and 30 mL/min hydrogen and 300 mL/min compressed air flow. The identities of the carboxylic acids were verified by the injection of authentic standards at a concentration of 50ng/µL. Retention indices were calculated in reference to an alkane standard mixture (C8-C20, Sigma-Aldrich).

***O*-AS relative comparison analysis**

To cross-compare *O*-AS levels among different accessions or genotypes, we extracted leaf or trichome *O*-AS using a method described by Gaquerel et al. (2010). Briefly, approximately 100 mg of ground leaf materials (without the midvein) or 50mg trichome materials were homogenized with 2 steel beads by GenoGrinder 2000 (SPEX SamplePrep) at 1100 strokes per minute for 30 seconds and then extracted with 1 mL extraction solution (50 mM acetate buffer, pH 4.8, containing 40% methanol spiked with sucrose monolaurate (Sigma) with final concentration of 10 ng/µL as an internal standard. The extraction was done using GenoGrinder 2000 (SPEX SamplePrep) with 1100 strokes per min for 15 minutes. After centrifugation at 13,200 rpm for 20 min at 4^{o}C, the supernatant was collected and centrifuged again. 100 µL of the supernatant was transferred to a HPLC vial and 1 µL supernatants were separated using a HPLC Dionex RSLC system (Dionex, Sunnyvale, USA) with a Dionex Acclaim RSLC 120 C-18 column (150 x 2.1 mm, 2.2 µm). The following binary gradient was applied: 0.5 min isocratic 90% A (deionized water, 0.1% (v/v) acetonitrile (Baker, HPLC grade), and 0.05% formic acid), 10% B (acetonitrile and 0.05%formic acid); 13 min linear gradient to 80% B; isocratic for 1.5 min. The flow rate was 400 µL/min. MS detection was carried out with the UHPLC/TOF-MS system (Bruker Daltonik, Bremen, Germany) operated in positive electrospray mode. Typical instrument settings were described by Gilardoni et al. (2011) with some modification: capillary voltage, 4500 V; dry gas temperature, 200 °C; dry gas flow, 10 L/min. Ions were detected from m/z 50 to 1400 at a repetition rate of 2 Hz. Mass calibration was performed using sodium formate clusters (10 mM solution of NaOH in 50/50% v/v isopropanol/water containing 0.2% formic acid). The peak areas were integrated using extracted ion traces for the sodium adduct [M+Na]+ of each individual *O*-AS in the QuantAnalysis software version 2.0 SP1 (Bruker Daltonics).The amount of each *O*-AS in plant tissue was normalized internal standard and the fresh weight of the tissue. Total *O*-AS was calculated by summing the normalized peak area of all 15 *O*-AS. The annotated 15 *O*-AS together with its m/z value and retention time (RT) is listed in Table S2.

Extraction and analysis of phytohormones, secondary metabolites

Phytohormone extraction was carried out as described previously by Gilardoni et al. (2011). Briefly, 0.1 g of frozen leaf tissue was homogenized with a Genogrinder 2000 (BTC and OPS Diagnostics). One

milliliter of ethylacetate spiked with [9,10-$^{2}H_2$]-dihydro-JA and [$^{13}C_6$]-JA-Ile was added to the samples. After vortexing, the samples were centrifuged for 20 min at 12,000g (4°C). The organic phase was collected and evaporated to dryness, which were subsequently reconstituted in 300 mL of 70% (v/v) methanol/water for analysis on a Bruker Elite EvoQ Triple quad-MS equipped with a HESI (heated electrospray ionization) ion source using the MRM transitions described in (Schäfer et al., 2016). Each phytohormone (JA, JA-Ile) was quantified by comparing its peak area with the peak area of its respective internal standard as described in Wu et al. (2007). Phytohormone levels were quantified per gram fresh mass (µg/gFM).

Nicotine and hydroxygeranyllinalool diterpene glycosides (HGL-DTGs) were extracted as described above for *O*-AS extraction. Analysis of these metabolites was done using an HPLC-DAD method described by Keinanen et al. (2001) with some modification. Briefly, after extraction, 1µL of the supernatants were injected into an Agilent 1100 HPLC (Agilent HPLC 1100 Series, Palo Alto, CA) installed with a Chromolith FastGradient RP-18 (5032 mm; Merck, Darmstadt, Germany) endcapped 50 x 2 mm HPLC column (Lot No. HX802433 Merck, Darmstadt, Germany) attached to a Gemini NX RP18, 3µm, 2 x 4.6 mm precolumn (Phenomenex, Aschaffenburg, Germany) with a column oven set at 40°C. The mobile phase consisted of a mix of solvent A (0.1 % formic acid and 0.1 % ammonium hydroxide solution in water (pH 3.5) and solvent B (methanol) was used in a gradient mode (time/concentration min/% for A: 0:00/100; 0.50/100; 6.50/20; 10:00/20; 15:00/100) with a flow rate 0.8 mL/min. Under these conditions, nicotine eluted at a retention time (RT) of 0.5 min (detected by UV absorbance at 260 nm. HGL-DTGs were detected by evaporative light scattering detector (ELSD) after HPLC separation at RT from 7.15 to 8.31 min. The peak areas were integrated using the Chromeleon software (Thermofisher) and nicotine in plant tissue was quantified using external dilution series of standard mixtures of nicotine. The peak areas were quantified to estimate total HGL-DTGs contents and normalized it to tissue fresh mass. The method was described previously by Kaur et al. (2010)

Ir-construct sequence of *NaBCKDE1*

GAAGATGTTGGTTTCGGTGGTGTCTTTCGTTGCACTACTGGATTAGCTGACCGATTTGGAAAACAG
AGAGTTTTTAACACTCCTTTATGTGAGCAGGGCATAGTTGGATTTGCTATTGGTCTGGCTGCAATG
GACAATCGAGCTATAGCAGAAATTCAATTTGCAGATTATATTTTTCCTGCTTTCGATCAGATCGTCA
ATGAAGCTGCGAAATTCAGATATAGGAGTGGTAATCAGTTCAACTGCGGAGGCTTAACTATAAGA
GCACCTTATGGAGCTGTTGGACATGGCGGGCATTACCACTCACAATCCCCTGAATCTTTCTTCTGCC
ATGTTCCTGGTATAAAGGTG

RNA extraction, cDNA synthesis and quantitative real-time PCR

Total RNA was extracted from approximately 50 mg of frozen leaf or trichome tissue with Trizol (Thermo scientific, 15596-026), followed by DNase-I treatment (Thermo Scientific) according to the manufacturer's instructions. The cDNA was synthesized from 2 µg of total RNA using RevertAid First Strand cDNA Synthesis Kit (Thermo scientific, K162). Quantitative real-time PCR was conducted with synthesized cDNA using the Takyon™ qPCR Kits for SYBR® assays (Eurogentec) and gene-specific primer pairs using Mx3005P PCR cycler (Stratagene). Relative gene expression was calculated from calibration curves obtained by analysis of dilution series of cDNA samples, and the values were normalized by the expression of housekeeping

gene *N. attenuata* actin 7. All reactions were performed using the following qPCR conditions: initial denaturation step of 95°C for 3 min, followed by 40 cycles each of 95°C for 10 s, 60°C for 20s and 72°C for 40s, followed by melting curve analysis of PCR products.

Primer sequences for SYBR-qPCR

NaBCKDE1B_For: 5'- GTATAAAGGTGGTCATCC-3'
NaBCKDE1B_Rev: 5'- GCAACATATAATCATCTTCA-3'
Na_Actin 7_For: 5'- TTCTTCGTCTGGACCTTGCT-3'
Na_Actin 7_Rev: 5'- ATCATGGATGGCTGGAAGAG-3'
NaBCKDE1A_1_For: 5'- CAATACATTATGGCTCTAAC -3'
NaBCKDE1A_1_Rev: 5'- GTCCATTTTCAGAGAATAAG -3'
NaBCKDE1A_2_For: 5'- GACCCAGTAACTAGATTCAG -3'
NaBCKDE1A_2_Rev: 5'- GTAAATACATGCTTAATTGG -3'
NaAT1_For: 5'- CTTATTCATCCAAGCAGTA -3'
NaAT1_Rev: 5'- AAGATAGTACCTCTTCTGG -3'
NaAT2_For: 5'- GTTCATCCAAAAGTTTTAC -3'
NaAT2_Rev: 5'- TCACAGCATGGACTAATG -3'
NaASH1_For: 5'- GAACTTTATGGCATAGTTG -3'
NaASH1_Rev: 5'- GTAGTAAACTAAGACGGGTAG -3'
NaASH2_For: 5'- GTTTTCTCTAAAGACGTCAC -3'
NaASH2_Rev: 5'- TGACGTAACAGTGATTCC -3'

Literature Cited

Gaquerel E, Heiling S, Schoettner M, Zurek G, Baldwin IT (2010) Development and validation of a liquid chromatography-electrospray ionization-time-of-flight mass spectrometry method for induced changes in *Nicotiana attenuata* leaves during simulated herbivory. Journal of Agricultural and Food Chemistry 58: 9418-9427

Gilardoni PA, Hettenhausen C, Baldwin IT, Bonaventure G (2011) *Nicotiana attenuata* LECTIN RECEPTOR KINASE1 suppresses the insect-mediated inhibition of induced defense responses during *Manduca sexta* herbivory. The Plant Cell 23: 3512-3532

Kaur H, Heinzel N, Schottner M, Baldwin IT, Galis I (2010) R2R3-NaMYB8 regulates the accumulation of phenylpropanoid-polyamine conjugates, which are essential for local and systemic defense against insect herbivores in *Nicotiana attenuata*. Plant Physiology 152: 1731-1747

Keinanen M, Oldham NJ, Baldwin IT (2001) Rapid HPLC screening of jasmonate-induced increases in tobacco alkaloids, phenolics, and diterpene glycosides in *Nicotiana attenuata*. Journal of Agricultural and Food Chemistry 49: 3553-3558

Schäfer M, Brütting C, Baldwin IT, Kallenbach M (2016) High-throughput quantification of more than 100 primary- and secondary-metabolites, and phytohormones by a single solid-phase extraction based sample preparation with analysis by UHPLC-HESI-MS/MS. Plant Methods 12: 30

Van Dam NM, Hare JD (1998) Biological activity of *Datura wrightii* glandular trichome exudate against

Manduca sexta larvae. Journal of Chemical Ecology 24: 1529-1549

Weinhold A, Baldwin IT (2011) Trichome derived *O*-acyl sugars are a first meal for caterpillars that tags them for predation. Proceedings of the National Academy of Sciences of the United States of America 108: 7855-7859

Wu J, Hettenhausen C, Meldau S, Baldwin IT (2007) Herbivory rapidly activates MAPK signaling in attacked and unattacked leaf regions but not between leaves of *Nicotiana attenuata*. The Plant Cell 19: 1096-1122